

THE SEPARATRIX ALGORITHMIC MAP: APPLICATION TO THE SPIN-ORBIT MOTION

IVAN I. SHEVCHENKO

*Pulkovo Observatory, Russian Academy of Sciences, Pulkovskoye ave. 65/1, St.Petersburg
196140, Russia; E-mail: iis@gao.spb.ru*

Abstract. The planar rotational motion of a non-symmetric satellite in an elliptic orbit is considered. A two-dimensional map is constructed, describing the motion in a vicinity of the separatrix of the synchronous spin-orbit resonance. This map is a generalization of Chirikov's separatrix map, in the sense that the asymmetry of perturbation is taken into account. Phase portraits of the generalized map perfectly reproduce well-known examples of surfaces of section (first computed by Wisdom *et al.* (Wisdom *et al.*, 1984), Wisdom (Wisdom, 1987)) of the phase space of spin-orbit coupling for non-symmetric natural satellites. Moreover, it provides a straightforward analytical description of the phase space: analysis of properties of the map allows one to precalculate, by means of compact analytical relations, the locations of resonances and chaos borders, the emergence of marginal resonances, and even to describe bifurcations of the synchronous resonance's center, though far from the separatrix.

1. Introduction

Equations of the nonlinear pendulum with periodic perturbations constitute an important paradigm in various fields of modern physics and mechanics. Consider the Hamiltonian

$$H = \frac{\mathcal{G}p^2}{2} - \mathcal{F} \cos \varphi + a \cos(\varphi - \tau) + b \cos(\varphi + \tau), \quad (1)$$

where $\tau = \Omega t + \tau_0$. The first two terms represent the Hamiltonian of the pendulum, while the two remaining ones the periodic perturbations. The variable φ is the pendulum angle (this angle measures deviation of the pendulum from the position of equilibrium), and τ is the phase angle of perturbation. The quantity Ω is the perturbation frequency and τ_0 is the initial phase of perturbation; p is the momentum; \mathcal{F} , \mathcal{G} , a , b are constants. In what follows, the Hamiltonian of the unperturbed pendulum is designated as H_0 , i.e. $H_0 = \frac{\mathcal{G}p^2}{2} - \mathcal{F} \cos \varphi$.

The motion in a vicinity of the separatrix of the Hamiltonian (1) in the symmetric case $a = b$ was considered by Chirikov (Chirikov, 1979). He showed that it is efficiently described by a map, which he called the whisker map. Now the term "separatrix map", hereafter SM, is customary for such kinds of maps. The SM in Chirikov's (Chirikov, 1979) form is a two-dimensional area-preserving map

$$\begin{aligned} w_{n+1} &= w_n - W \sin \tau_n, \\ \tau_{n+1} &= \tau_n + \lambda \ln \frac{32}{|w_{n+1}|} \pmod{2\pi}, \end{aligned} \quad (2)$$

where w denotes the relative (with respect to the separatrix value) pendulum energy $w = \frac{H_0}{\mathcal{F}} - 1$, and τ is the phase of perturbation. Constants λ and W are parameters:



λ is the ratio of Ω , the perturbation frequency, to $\omega_0 = (\mathcal{F}\mathcal{G})^{1/2}$, the frequency of the small-amplitude pendulum oscillations; and

$$W = \frac{a}{\mathcal{F}} \lambda (A_2(\lambda) + A_2(-\lambda)) = 4\pi \frac{a}{\mathcal{F}} \lambda^2 \operatorname{csch} \frac{\pi \lambda}{2}, \quad (3)$$

where

$$A_2(\lambda) = 4\pi \lambda \frac{\exp \frac{\pi \lambda}{2}}{\sinh(\pi \lambda)} \quad (4)$$

is the Melnikov–Arnold integral as defined in Refs. (Chirikov, 1979; Lichtenberg and Lieberman, 1987; Shevchenko, 1998). One iteration of the SM (2) corresponds to one period of the pendulum rotation, or a half-period of its libration.

In this paper, the separatrix algorithmic map (SAM) is constructed for the motion in a vicinity of the separatrix of the Hamiltonian (1). This map is a generalization of Chirikov’s SM (2), in the sense that the asymmetry of perturbation is taken into account. It constitutes an algorithm containing conditional transfer statements. Besides, a regular projection algorithm (RPA) is proposed, which allows one to construct phase portraits of the motion at customary sections of phase space.

The Hamiltonian (1) emerges in a number of mechanical and physical problems. The reason for such universality is that the nonlinear pendulum provides a model of the nonlinear resonance under very general conditions (Chirikov, 1979; Lichtenberg and Lieberman, 1987). In this general setting, the phase angle of the model pendulum has the meaning of the resonant phase angle.

The SAM is applied here to the problem of the resonant rotational motion of a non-symmetric satellite in an elliptic orbit. Performance of the SAM and RPA is checked in comparisons with direct numeric integrations of the original system (1). It is shown that the theory of the SAM provides a straightforward analytical description of the structure of phase space of the near-separatrix motion.

2. The Separatrix Algorithmic Map

The separatrix map in the case of asymmetric perturbation, i.e. $a \neq b$ in Eq. (1), is different from that in the symmetric case, since the energy increments are different for prograde and retrograde motions of the model pendulum. (Henceforth the motion is called “prograde” or “retrograde” if the increase in φ with time is respectively positive or negative.) Taking this difference into account, let us write down the following algorithm

$$\begin{aligned} &\text{if } w_n < 0 \text{ and } W = W^- \text{ then } W = W^+, \\ &\text{if } w_n < 0 \text{ and } W = W^+ \text{ then } W = W^-; \\ &w_{n+1} = w_n - W \sin \tau_n, \\ &\tau_{n+1} = \tau_n + \Delta_{n+1} \tau \pmod{2\pi}; \end{aligned} \quad (5)$$

where $\Delta_{n+1}\tau$, which is approximately equal to $\lambda \ln \frac{32}{|w_{n+1}|}$ (as it is adopted for the ordinary SM (2)), is defined in a more exact sense below, and W^+ , W^- denote the values of the parameter W for the prograde and retrograde motions respectively. In case of asymmetric perturbation these values are different.

The algorithm (5) constitutes the separatrix algorithmic map (SAM). Its essence is in taking into account alternations of the parameter W . The latter one alternates when the direction of motion alternates. This takes place when rotation changes to libration and when the motion is librational. The algorithm (5) does not contain conditions with $w_n > 0$, because the direction of motion does not change when they hold.

An important property of the original SM (2) is that it maps the motion asynchronously: the relative energy w is mapped at $\varphi = \pm\pi$, while the phase angle of perturbation τ is mapped at $\varphi = 0$. The SAM (5) retains this asynchronism. The procedure of synchronization of the SM (2) to the unified surface of section $\varphi = 0$ is described in Ref. (Shevchenko, 1998). An analogous procedure of synchronization of the SAM (5) can be also derived. It is more complicated. However, it is not needed in what follows and is not presented here.

In order to find expressions for W^+ , W^- , one should integrate the increment of energy per one iteration of the map, following the usual procedure (Chirikov, 1979), but making it separately for prograde and retrograde directions of motion. This gives

$$W^+(\lambda, \eta) = \frac{a}{\mathcal{F}} \lambda (A_2(\lambda) + \eta A_2(-\lambda)), \tag{6}$$

$$W^-(\lambda, \eta) = \frac{a}{\mathcal{F}} \lambda (\eta A_2(\lambda) + A_2(-\lambda)), \tag{7}$$

where $\eta = \frac{b}{a}$; the function $A_2(\lambda)$ is given by Eq. (4).

One should be aware that the expression for the increment of the phase τ in the ordinary SM (2) is an approximation. It is valid for a low strength of perturbation, i.e. for $W \ll 1$. According to Ref. (Shevchenko, 1998), if the perturbation is not weak, one can improve the performance of the map by means of replacing the logarithmic approximation of the phase increment by its exact value, which depends on what side of the line of the unperturbed separatrix the motion takes place. Making this replacement, one obtains the expression for the exact increment:

$$\Delta_{n+1}\tau = \begin{cases} 2\lambda \mathbf{K} \left(\left(1 + \frac{w_{n+1}}{2}\right)^{1/2} \right), & \text{if } w_{n+1} < 0; \\ 2\lambda \left(1 + \frac{w_{n+1}}{2}\right)^{-1/2} \mathbf{K} \left(\left(1 + \frac{w_{n+1}}{2}\right)^{-1/2} \right), & \text{if } w_{n+1} > 0; \end{cases} \tag{8}$$

where $\mathbf{K}(k)$ is the elliptic integral of the first kind. The first line in Eq. (8) corresponds to libration of the model pendulum, while the second one to its rotation. In the algorithm (5), henceforth the exact expression (8) is used.

3. The Regular Projection Algorithm

The SAM maps the motion of the system (1) on the plane (τ, w) at fixed values of the resonant phase angle φ equal to 0 and $\pm\pi$ (as noted in Section 2, the mapping is asynchronous). When Poincaré sections are constructed numerically in applied problems, it is customary to use another plane, namely the plane (φ, p) taken at a fixed value of the phase angle of perturbation, e.g. $\tau = 0 \pmod{2\pi}$.

Consider the problem how the section of the second kind can be found with the help of the separatrix map. In order to characterize the current state of the system, described by the SAM, introduce temporary designations $w = w_n$, $\tau = \tau_n$; and $\Delta\tau = \tau_n - \tau_{n-1}$. The value of W , which specifies the current prograde/retrograde state of the system, is taken at the next iteration $n + 1$. The matter is that the values of the variables w_n and τ_n , given by the SAM (5), as well as by the usual SM (2), correspond to different instants of time (the property of asynchronism, noted already in Section 2). The phase τ_n is mapped with a delay in relation to the relative energy w_n . The delay is equal to a half-period of rotation, or a quarter-period of libration of the model pendulum. Due to this delay, the value of W in the formula for w_{n+1} in the SAM (5) specifies the prograde/retrograde state of the system at the preceding instant τ_n ; or, inversely, the state of the system at τ_n is determined by the value of W in the formula for w_{n+1} , i.e. at the next iteration.

Let us find the phase point which is connected with the position of the system at the current instant τ (corresponding to $\varphi = 0$) by a trajectory backwards in time, and which is situated at the nearest surface $\tau = 0 \pmod{2\pi}$. The trajectory is assumed to be regular and possessing energy w . For convenience, the current instant τ is taken moduli 2π , while the increment $\Delta\tau$ is not. If $\Delta\tau \leq \tau$, there are no intersections with the plane of interest on the open interval of time backwards in relation to the current state, and no projection is made therefore at such an iteration of the map. Otherwise, the projection to the nearest surface $\tau = 0 \pmod{2\pi}$ is given by the formulae

$$\varphi = \begin{cases} \varphi(t = -\frac{\tau}{\Omega}), & \text{if } W = W^+ \text{ (prograde),} \\ -\varphi(t = -\frac{\tau}{\Omega}), & \text{if } W = W^- \text{ (retrograde),} \end{cases} \quad (9)$$

$$p = \begin{cases} p(t = -\frac{\tau}{\Omega}), & \text{if } W = W^+ \text{ (prograde),} \\ -p(t = -\frac{\tau}{\Omega}), & \text{if } W = W^- \text{ (retrograde),} \end{cases} \quad (10)$$

where $\varphi(t)$ and $p(t)$ represent the explicit solution of equations of the unperturbed nonlinear pendulum (cf. e.g. (Wisdom, 1985)):

$$\begin{aligned} \cos \varphi(t) &= 1 - 2k^2 \operatorname{sn}^2(\omega_0 t), \\ \sin \varphi(t) &= 2k \operatorname{sn}^2(\omega_0 t) (1 - k^2 \operatorname{sn}^2(\omega_0 t))^{1/2}, \\ p(t) &= \frac{2\omega_0 k}{G} \operatorname{cn}(\omega_0 t), \end{aligned} \quad (11)$$

for libration, and

$$\begin{aligned} \cos \varphi(t) &= \operatorname{cn}^2(\omega_r t) - \operatorname{sn}^2(\omega_r t), \\ \sin \varphi(t) &= 2 \operatorname{sn}(\omega_r t) \operatorname{cn}(\omega_r t), \\ p(t) &= \frac{2\omega_r}{g} \operatorname{dn}(\omega_r t), \end{aligned} \tag{12}$$

for rotation; sn , cn , dn are Jacobi elliptic functions, $\omega_r = \frac{\omega_0}{k}$,

$$k = \begin{cases} (1 + \frac{w}{2})^{1/2}, & \text{if } w < 0 \text{ (libration),} \\ (1 + \frac{w}{2})^{-1/2}, & \text{if } w > 0 \text{ (rotation),} \end{cases} \tag{13}$$

is the elliptic modulus (compare with Eq. (8)).

One iteration of the SAM can produce several (or even many) projected points. To find all projected points for a given iteration, one should employ the following algorithm

```

while  $\Delta\tau > \tau$  do
  evaluate  $\varphi, p$  by Eqs. (9, 10)
   $\tau := \tau + 2\pi$ 
end do
    
```

Note that the input value of τ is taken moduli 2π , while the increment $\Delta\tau$ and consequent values of τ are not. In words, the contents of the algorithm are as follows. It is verified whether the intersection condition $\Delta\tau > \tau$ is valid, and if yes, a projection is made. Then the interval τ is incremented by 2π and it is verified whether the intersection condition is still valid. If yes, the projection is accomplished once more with the new value of τ , and one more phase point on the plane (φ, p) , $\tau = 0 \pmod{2\pi}$, is found. The cycle is repeated until $\Delta\tau \leq \tau$.

The described procedure is applied at each iteration of the SAM. Since it is based on the regular approximation of the motion on small time scales, it is called henceforth the regular projection algorithm (RPA).

4. The Spin-Orbit Resonance Problem

One of straightforward applications of the SAM concerns the planar resonant rotational motion of a non-symmetric satellite in an elliptic orbit. In this Section, it is shown how the SAM can be used to describe the motion in a vicinity of the separatrix of the synchronous spin-orbit resonance.

The orbit of the satellite is assumed to be a fixed ellipse. The vector of the angular momentum coincides with the axis of the maximum moment of inertia and is perpendicular to the orbit plane (the rotational motion is planar). The Hamiltonian

TABLE I
Satellites. Inertial, orbital and SAM parameters

Satellite	ω_0	e	Ref.	λ	W^+	W^-
Phobos	0.86	0.015	Wisdom, 1987	1.163	-0.286	0.0336
Deimos	0.81	0.0005	Wisdom, 1987	1.235	-0.00962	0.00118
Amalthea	1.14	0.003	Wisdom, 1987	0.877	-0.0509	0.00408
Janus	0.14 ^{1/2}	0.009	Goźdz., 1997	2.673	-0.0850	0.0121
Epimetheus	0.87	0.007	Goźdz., 1997	1.149	-0.133	0.0155
Pandora	0.93	0.004	Goźdz. & Macie. 1995	1.075	-0.0749	0.00818
Prometheus	1.17	0.004	Goźdz. & Macie. 1995	0.855	-0.0668	0.00503
Bif. case	0.50	0.01	-	2	-0.152	0.0214

of the problem (Wisdom *et al.*, 1984; Celletti, 1990), if the terms beyond first order in the eccentricity are ignored, has the form

$$H = \frac{y^2}{2} - \frac{\omega_0^2}{4} \cos(2x - 2t) - \frac{7e\omega_0^2}{8} \cos(2x - 3t) + \frac{e\omega_0^2}{8} \cos(2x - t), \quad (14)$$

where x is the orientation of the satellite, i.e. the angle between the axis of the minimum moment of inertia and the line of apsides; $y = \dot{x} \equiv \frac{dx}{dt}$, and t is time.

The parameters are: the inertial parameter $\omega_0 = \left(\frac{3(B-A)}{C}\right)^{1/2}$, where $A < B < C$ are the principal moments of inertia of the satellite; and the eccentricity e of the satellite's orbit. The time unit is equal to $\frac{1}{2\pi}$ of the orbital period.

By means of the canonical transformation $p = \frac{y-1}{2}$, $\varphi = 2(x - t)$, the Hamiltonian (14) is reducible to the paradigm (1) of the perturbed pendulum:

$$H = 2p^2 - \frac{\omega_0^2}{4} \cos \varphi - \frac{7e\omega_0^2}{8} \cos(\varphi - t) + \frac{e\omega_0^2}{8} \cos(\varphi + t). \quad (15)$$

The motion in a vicinity of the separatrix of the Hamiltonian (15) is described by the SAM (5). Comparing Eqs. (1) and (15), one has $\mathcal{F} = \frac{\omega_0^2}{4}$, $\mathcal{G} = 4$, $\Omega = 1$, $a = -\frac{7e\omega_0^2}{8}$, $b = \frac{e\omega_0^2}{8}$. Thus the SAM parameters $\lambda = \frac{1}{\omega_0}$ and W^+ , W^- , given by Eqs. (6, 7), are determined by the inertial parameter ω_0 and by the eccentricity e . Since $a = -7b$ (i.e. $\eta = -1/7$) the asymmetry of perturbation is intermediate; if $\lambda > 1$ then $W^+ \approx -7W^-$.

Available data on the inertial and orbital parameters of natural satellites of planets, as well as the calculated values of the SAM parameters, are presented in Table 1. In Fig. 1, the main chaotic layer computed by the SAM-RPA is shown on the plane (x, y) , $t = 0 \pmod{2\pi}$, for the case of Phobos. Note that the transformation from

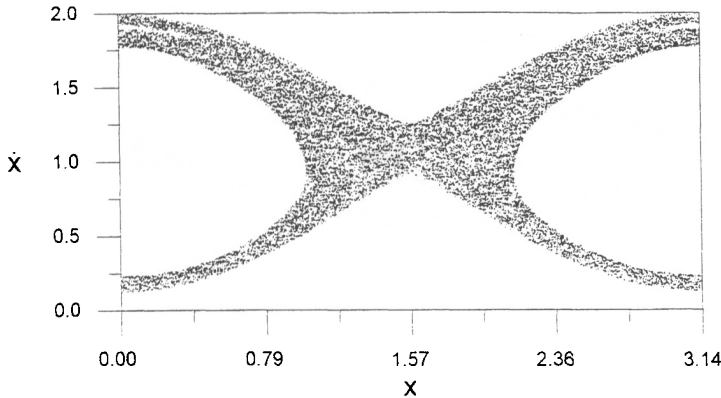


Fig. 1. Phobos. The main chaotic layer on the phase plane $(x, y), t = 0 \pmod{2\pi}$. Computed by means of the SAM-RPA.

φ, p to x, y at this plane is $x = \frac{\varphi}{2}, y = 1 + 2p$. In order to check the performance of the SAM-RPA, I constructed the corresponding section of phase space by means of a direct numeric integration and compared it to the phase portrait in Fig. 1. The integration was performed by the 8th order Dormand-Prince technique (Hairer *et al.*, 1987) with the local tolerance set to 10^{-10} . Close, almost exact agreement between the SAM-RPA and the integration was observed. What is more, there is also close agreement with the corresponding surface of section obtained by a direct integration by Wisdom (Wisdom, 1987), cf. Fig. 1 of Ref. (Wisdom, 1987). Note that the SAM-RPA is a hundred times faster than usual numeric integrations.

Close agreement between the SAM-RPA and numeric integrations was observed for all satellites in Table 1. In Figs. 2, 3, the phase portraits are presented for Deimos and Janus, for which the surfaces of section were originally obtained by means of direct integrations by Wisdom (Wisdom, 1987) and Goździewski (1997); see Fig. 3 of Ref. (Wisdom, 1987) (Deimos) and Fig. 5a of Ref. (Goździewski, 1997) (Janus; note that the coordinate system in the latter figure is different).

Apart from fast construction of phase portraits, the SAM provides useful theoretical advantages in description of the phase space structure. Consider the location of spin-orbit resonances, e.g. the half-integer resonances $1/2$ and $3/2$. One has for the time averaged derivatives: $\langle \dot{\varphi} \rangle = 2\langle y \rangle - 2$; therefore, these resonances both correspond to an integer resonance of the SAM. The resonance $1/2$ corresponds to the retrograde, while $3/2$ to the prograde resonant rotation of the model pendulum. This resonant rotation has winding number $Q = 1/\langle \dot{\varphi} \rangle = \pm 1$. If, say, $\langle y \rangle = 5/2$ then $Q = 1/3$.

The elliptic modulus $k^{(Q)}$ of the motion in the center of a resonance with winding number Q can be found by means of numeric solution of the equation

$$\lambda k^{(Q)} K(k^{(Q)}) = \pi|Q|, \tag{16}$$

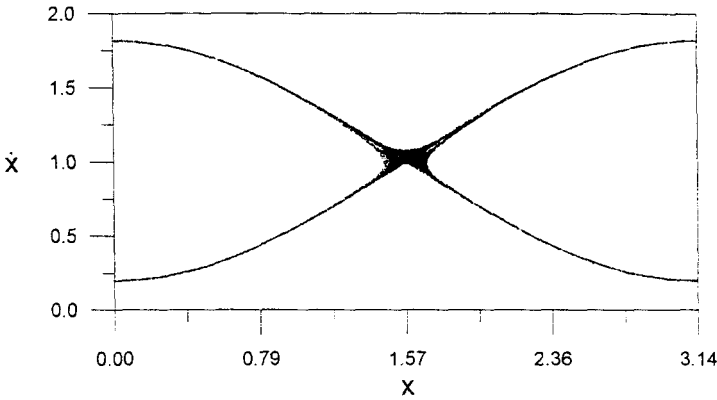


Fig. 2. The same for Deimos.

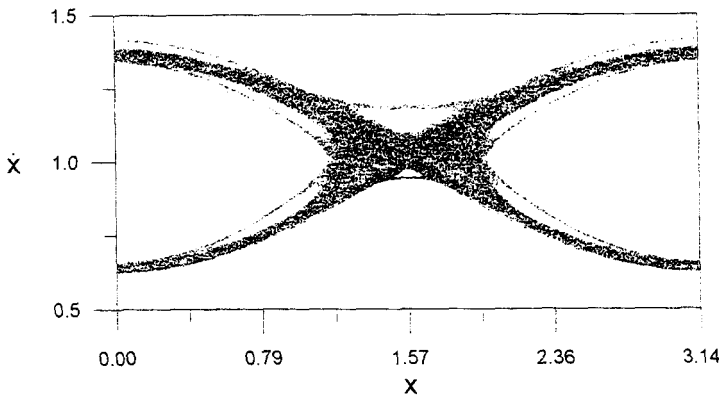


Fig. 3. The same for Janus.

following from Eq. (8); $\lambda = \frac{1}{\omega_0}$. It is efficiently solved by iterations. Then the energy deviation is $w^{(Q)} = 2 \left(\left(k^{(Q)} \right)^{-2} - 1 \right)$. On the other hand, the expression for H_0 (cf. Eq. (1)) is reducible to the relation

$$y = 1 \pm \frac{\omega_0}{2^{1/2}} (1 + w + \cos \varphi)^{1/2}. \tag{17}$$

The sign plus or minus refers to the prograde and retrograde motion respectively. In the coordinate x , the centers of resonances are located at $x = \pi/2$ (resonance 1/2) and at $x = 0$ (resonance 3/2), both mod π . Since $\varphi = 2x$ at $t = 0$, one has, via Eq. (17), the locations of centers of resonances 1/2 and 3/2 in the coordinate y :

$$\begin{aligned} y_{1/2} &= 1 - \frac{\omega_0}{2^{1/2}} \left(w^{(1)} \right)^{1/2}, \\ y_{3/2} &= 1 + \frac{\omega_0}{2^{1/2}} \left(2 + w^{(1)} \right)^{1/2}. \end{aligned} \tag{18}$$

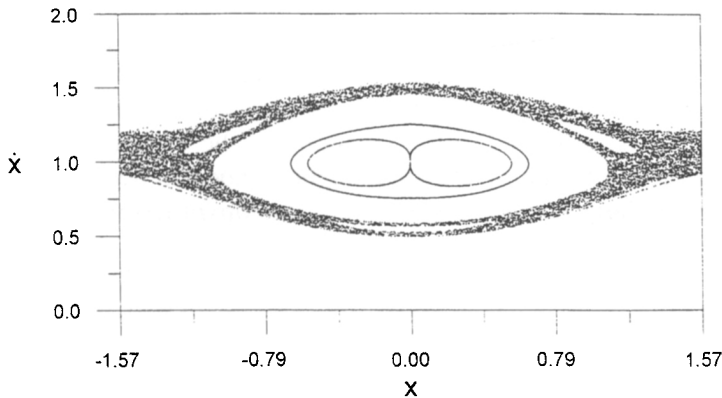


Fig. 4. A phase portrait in case of the resonance $\lambda = 2$ (see Table 1). Computed by means of the SAM–RPA. The period-doubling bifurcation of the synchronous resonance (the “ ∞ ” librational invariant curve in the center) is evident. Note that the coordinate x is shifted for convenience.

Evaluations of $y_{1/2}$, $y_{3/2}$ by Eqs. (16, 18) can be compared with results (Wisdom *et al.*, 1984, Fig. 3), obtained by localization of the resonances by a direct numeric integration. Good correspondence is observed.

The localization of resonances gives just one example of the SAM theory applications. Besides, this theory allows one to precalculate locations of chaos borders on the phase plane; to predict the emergence of marginal resonances (i.e. prominent intermittent behaviour, see Ref. (Shevchenko, 1998)). Consider the external borders of the chaotic layer. The separatrix map can be linearized in w to give the standard map; then the locations of the borders follow from conditions on the criticality of the parameter of the standard map (Chirikov, 1979). These considerations, as well as conditions for the emergence of marginal resonances (Shevchenko, 1998), are straightforwardly generalized to the case of the SAM.

The SAM allows one even to describe bifurcations of the synchronous resonance’s center. In Fig. 4, a phase portrait in case of the resonance $\lambda = 2$ between the perturbation frequency and the frequency of the small-amplitude pendulum oscillations is presented. The relevant data of the model are in Table 1. The main chaotic layer and librational invariant curves near the center of the synchronous resonance are shown. The period-doubling bifurcation of the resonance’s center clearly manifests itself, though the SAM is presumed to describe behaviour in a vicinity of the separatrix.

5. Conclusions

In this paper, the separatrix map (SM) in Chirikov’s (Chirikov, 1979) form, describing the motion in a vicinity of the separatrix of the nonlinear resonance, is generalized to the case of asymmetric perturbation. The new map (5) is an algorithm containing conditional transfer statements.

Introduction of this separatrix algorithmic map (SAM) expands the area of applications of the SM. In particular, the SAM is directly applicable to the problem of the planar rotational dynamics of a non-symmetric satellite in an elliptic orbit. The motion in a neighbourhood of the separatrix of the synchronous spin-orbit resonance is reducible to the SAM. This neighbourhood is not at all a narrow region. It is usually large enough to engulf most important resonances other than the synchronous one.

The SAM, together with the regular projection algorithm (RPA), reproduces phase portraits of the motion which are in close agreement with well-known surfaces of section obtained by Wisdom et al. (Wisdom *et al.*, 1984), Wisdom (Wisdom, 1987), Goździewski (Goździewski, 1997) and others by means of numeric integration of equations of the rotational motion of non-symmetric natural satellites. The application of the SAM–RPA provides a hundred times advantage in the computation speed. The SAM theory allows one to analytically precalculate locations of resonances and chaos borders.

Acknowledgements

The author is grateful to Christos Efthymiopoulos for useful remarks and comments on the manuscript. This work was partially supported by the Russian Foundation of Fundamental Research under Grant 97-01-01176.

References

- A. Celletti: 1990, Analysis of resonances in the spin-orbit problem in Celestial Mechanics: The synchronous resonance (Part I), *ZAMP*, **41**, 174–204.
- B. V. Chirikov: 1979, A universal instability of many-dimensional oscillator systems, *Phys. Reports*, **52**, 263–379.
- K. Goździewski: 1997, Rotational dynamics of Janus and Epimetheus, in: *Dynamics and Astrometry of Natural and Artificial Celestial Bodies*, I. M. Wytrzyszczak et al., eds, Kluwer Academic Publishers, Dordrecht, 269–274.
- K. Goździewski and A. J. Maciejewski: 1995, On the gravitational fields of Pandora and Prometheus, *Earth, Moon and Planets*, **69**, 25–50.
- E. Hairer, S. P. Nørsett and G. Wanner: 1987, *Solving Ordinary Differential Equations I: Nonstiff Problems*, Springer-Verlag, Berlin.
- A. J. Lichtenberg and M. A. Leiberman: 1992, *Regular and Chaotic Dynamics*, Springer-Verlag, New York.
- I. I. Shevchenko: 1998, Marginal resonances and intermittent behaviour in the motion in the vicinity of a separatrix, *Physica Scripta*, **57**, 185–191.
- J. Wisdom: 1985, A perturbative treatment of motion near the 3/1 commensurability, *Icarus*, **63**, 272–289.
- J. Wisdom: 1987, Rotational dynamics of irregularly shaped natural satellites, *Astron. J.*, **94**, 1350–1360.
- J. Wisdom, S.J. Peale and F. Mignard: 1984, The chaotic rotation of Hyperion, *Icarus*, **58**, 137–152.